

Supporting Information

Highly Efficient and Selective Recovery of Rare Earth Elements Using Mesoporous Silica Functionalized by Preorganized Chelating Ligands

Yimu Hu,^{a,b,c} Elisabeth Drouin,^{a,c} Dominic Larivière,^{*a,c} Freddy Kleitz,^{*a,b,d}
and Frédéric-Georges Fontaine^{*a,c}

^aDepartment of Chemistry, Université Laval, Québec, G1V 0A6, QC, Canada

E-mail: dominic.lariviere@chm.ulaval.ca; frederic.fontaine@chm.ulaval.ca

^bCentre de Recherche sur les Matériaux Avancés (CERMA), Université Laval, Québec, G1V 0A6, QC, Canada

^cCentre en Catalyse et Chimie Verte (C3V), Université Laval, Québec, G1V 0A6, QC, Canada

^d Department of Inorganic Chemistry – Functional Materials, Faculty of Chemistry, University of Vienna, 1090 Vienna, Austria. E-mail: freddy.kleitz@univie.ac.at

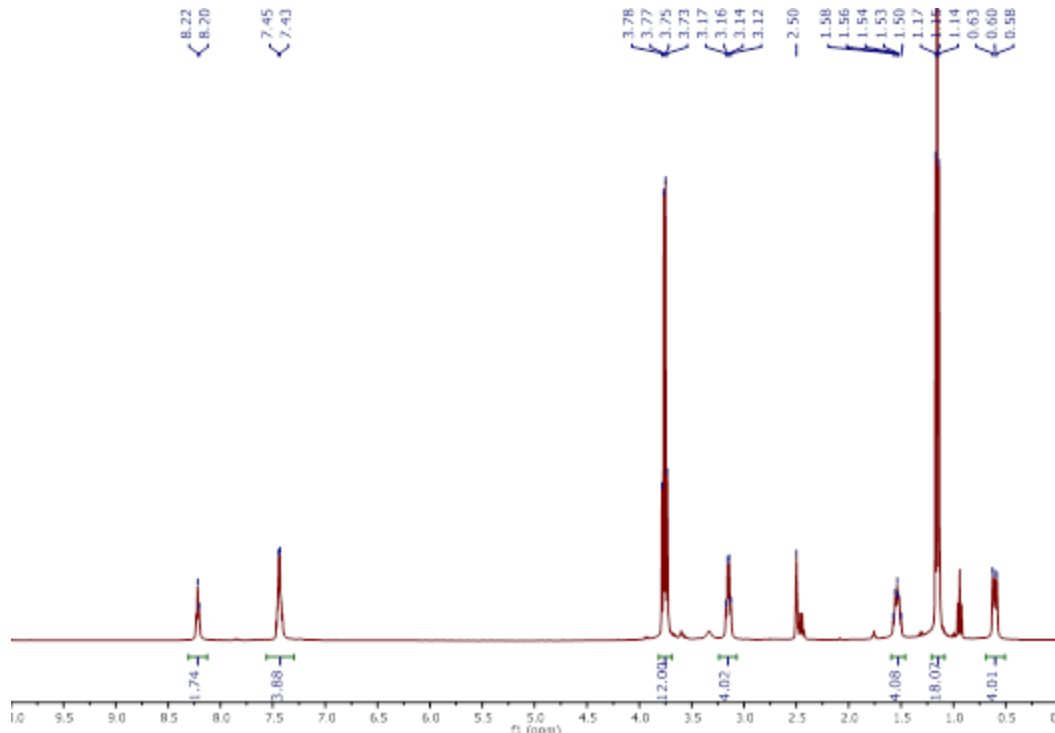


Figure S1. ^1H NMR of 1,2-PA-APTS (DMSO- d_6 , 400 MHz).

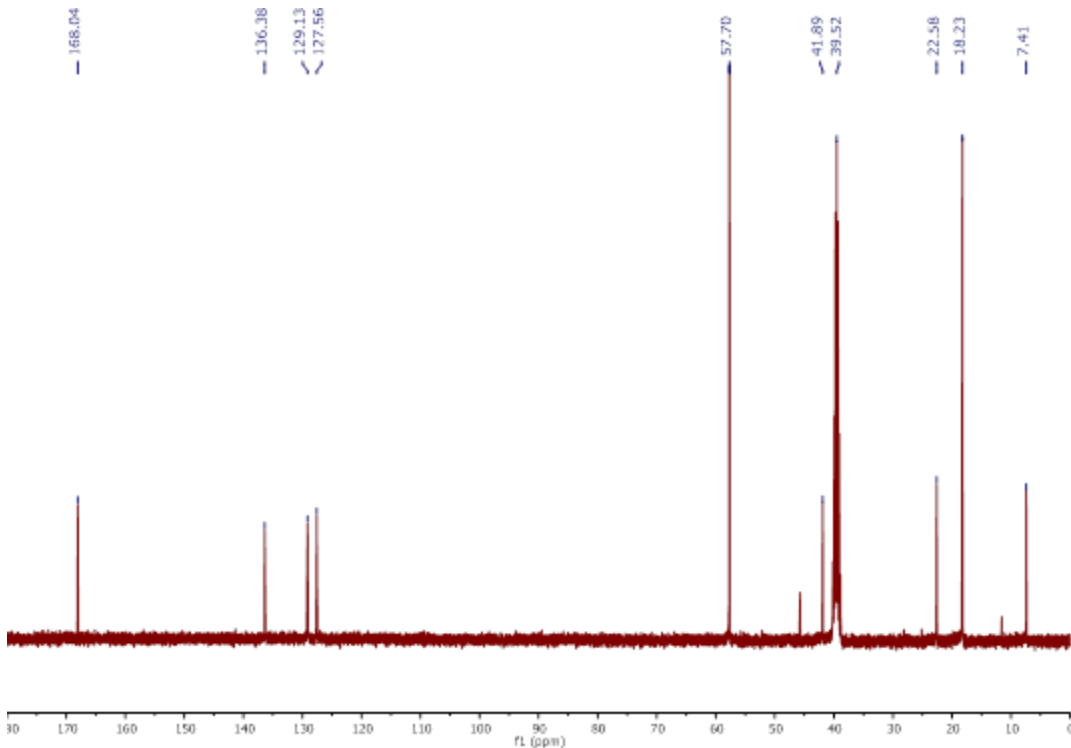


Figure S2. $^{13}\text{C}\{^1\text{H}\}$ NMR of 1,2-PA-APTS (DMSO- d_6 , 100 MHz).

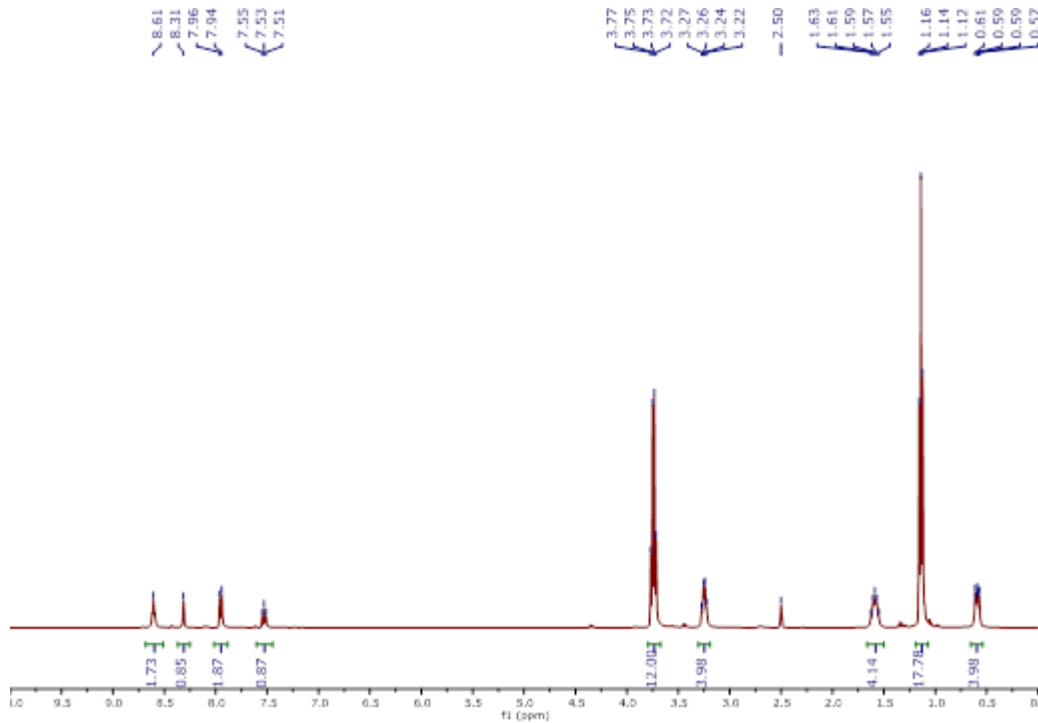


Figure S3. ^1H NMR of 1,3-PA-APTS (DMSO- d_6 , 400 MHz).

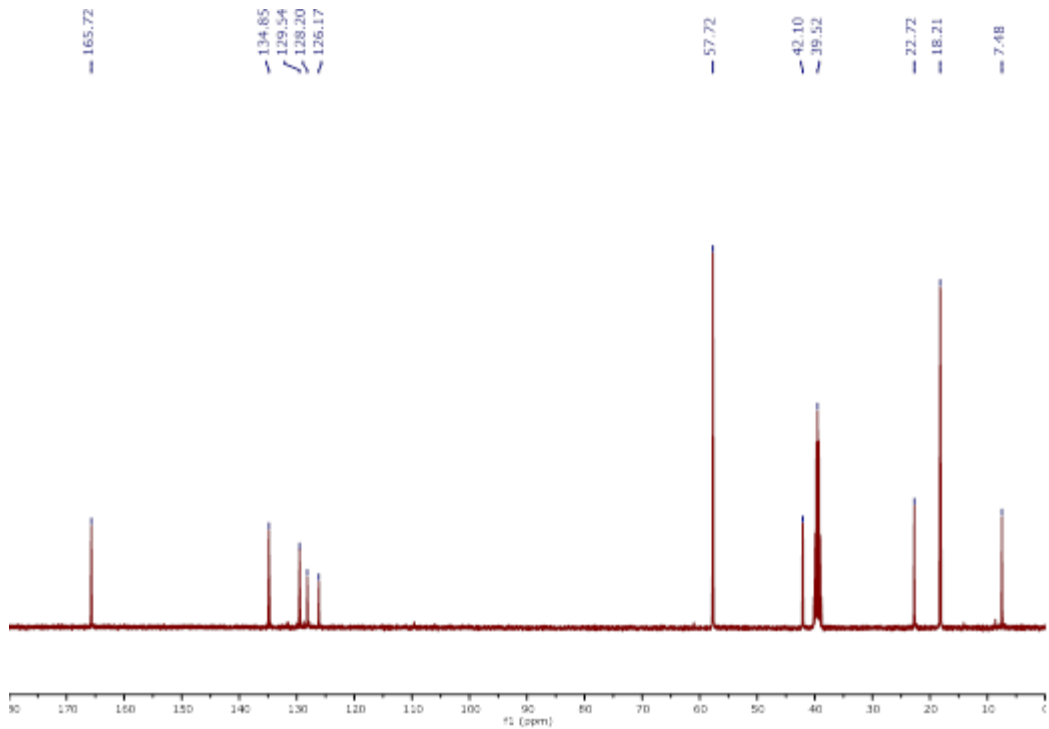


Figure S4. $^{13}\text{C}\{\text{H}\}$ NMR of 1,3-PA-APTS (DMSO- d_6 , 100 MHz).

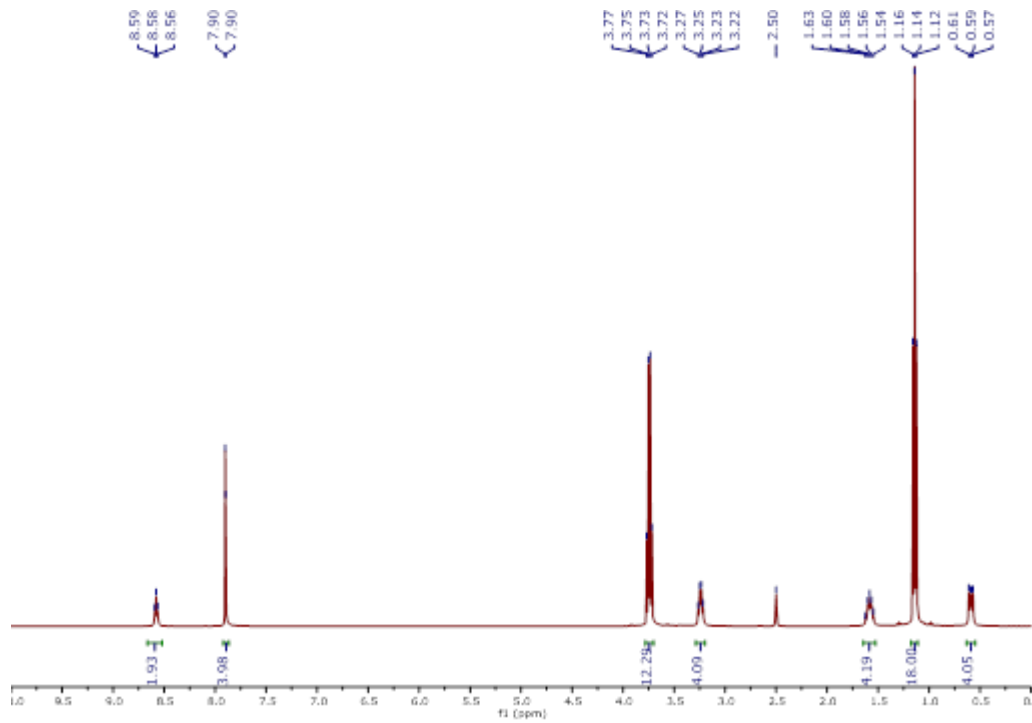


Figure S5. ^1H NMR of 1,4-PA-APTS (DMSO- d_6 , 400 MHz).

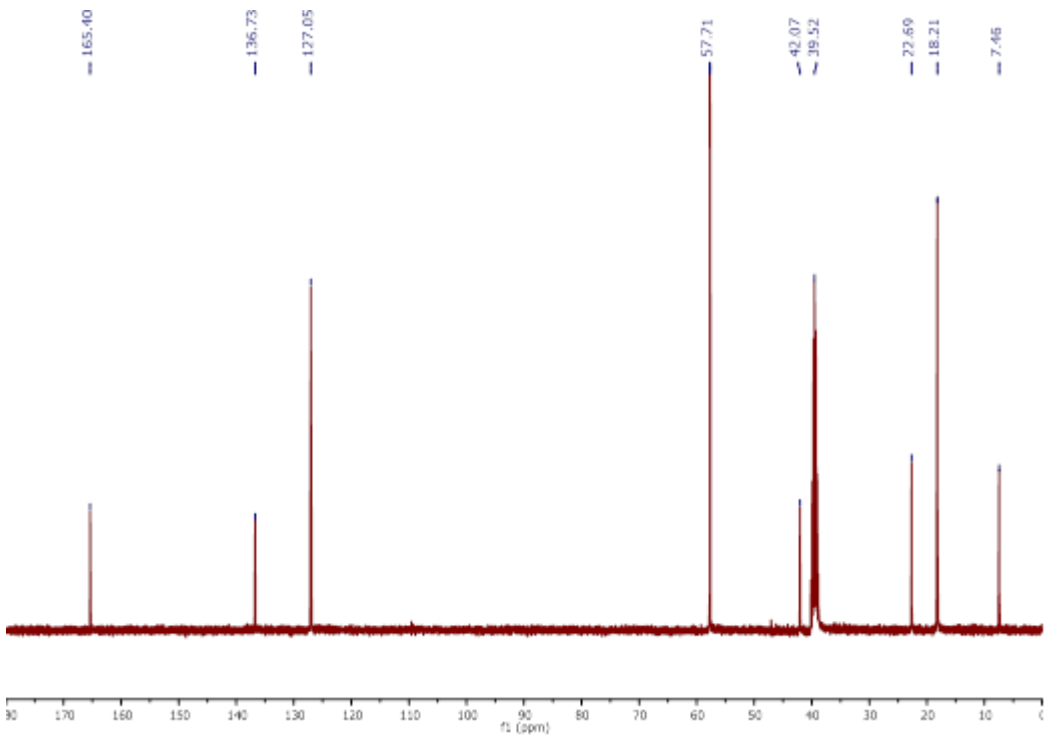


Figure S6. $^{13}\text{C}\{\text{H}\}$ NMR of 1,4-PA-APTS (DMSO- d_6 , 100 MHz).

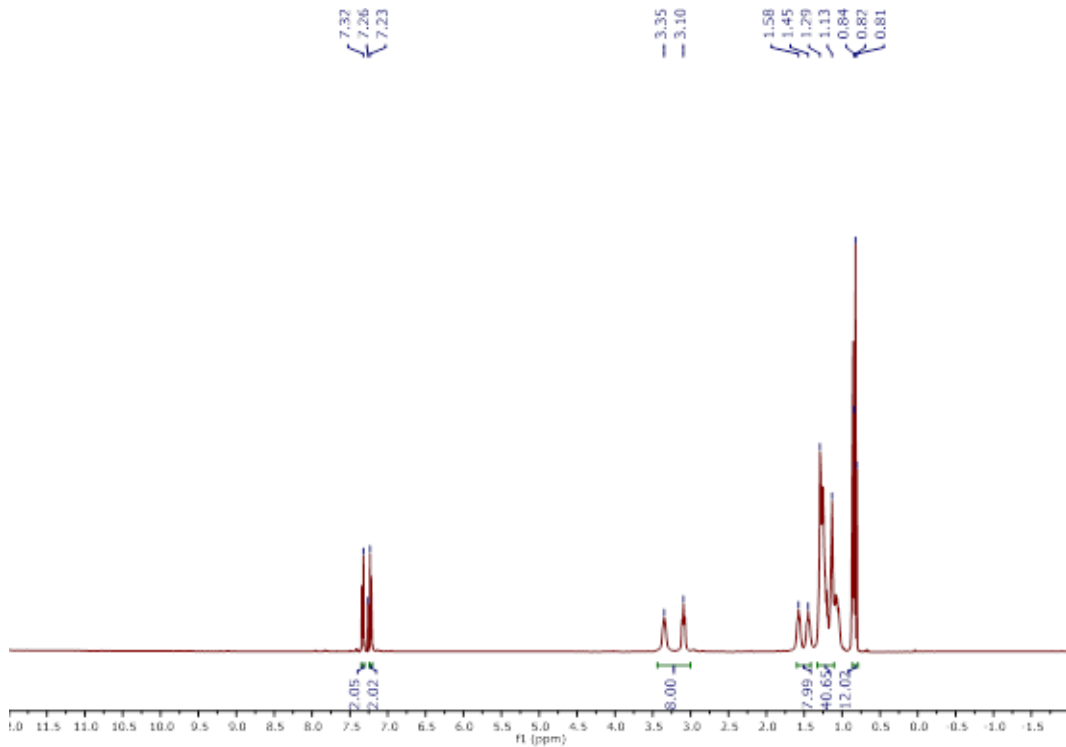


Figure S7. ^1H NMR of 1,2-DOPA (*chloroform-d*, 400 MHz).

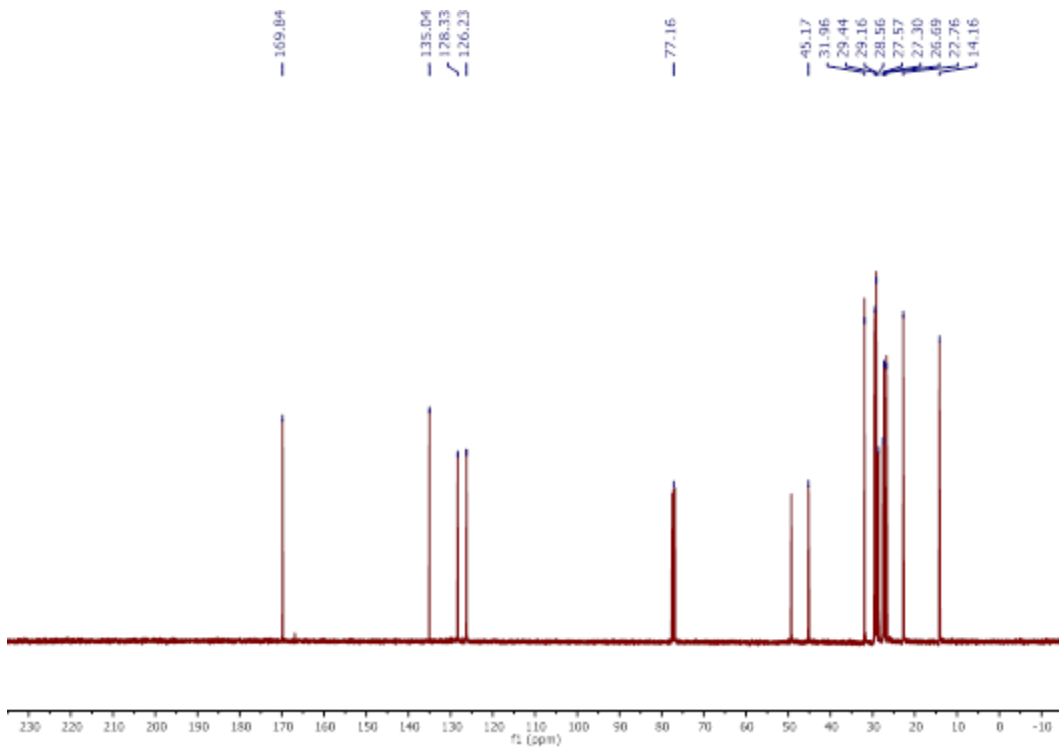


Figure S8. $^{13}\text{C}\{^1\text{H}\}$ NMR of 1,2-DOPA (*chloroform-d*, 100 MHz).

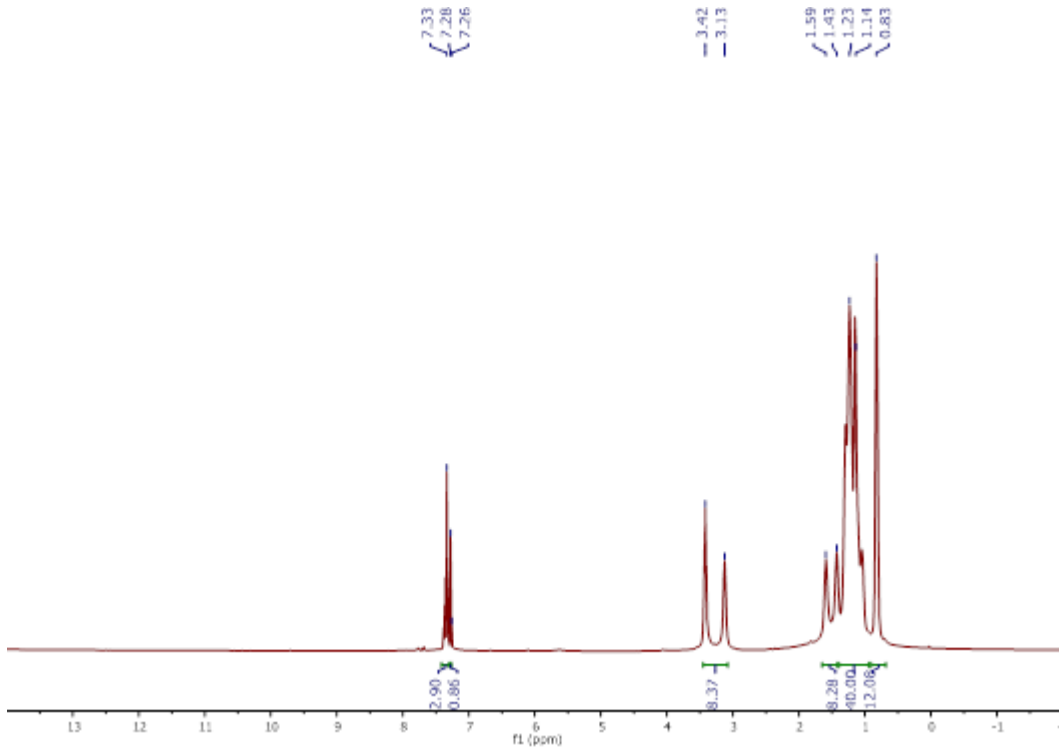


Figure S9. ^1H NMR of 1,3-DOPA (*chloroform-d*, 400 MHz).

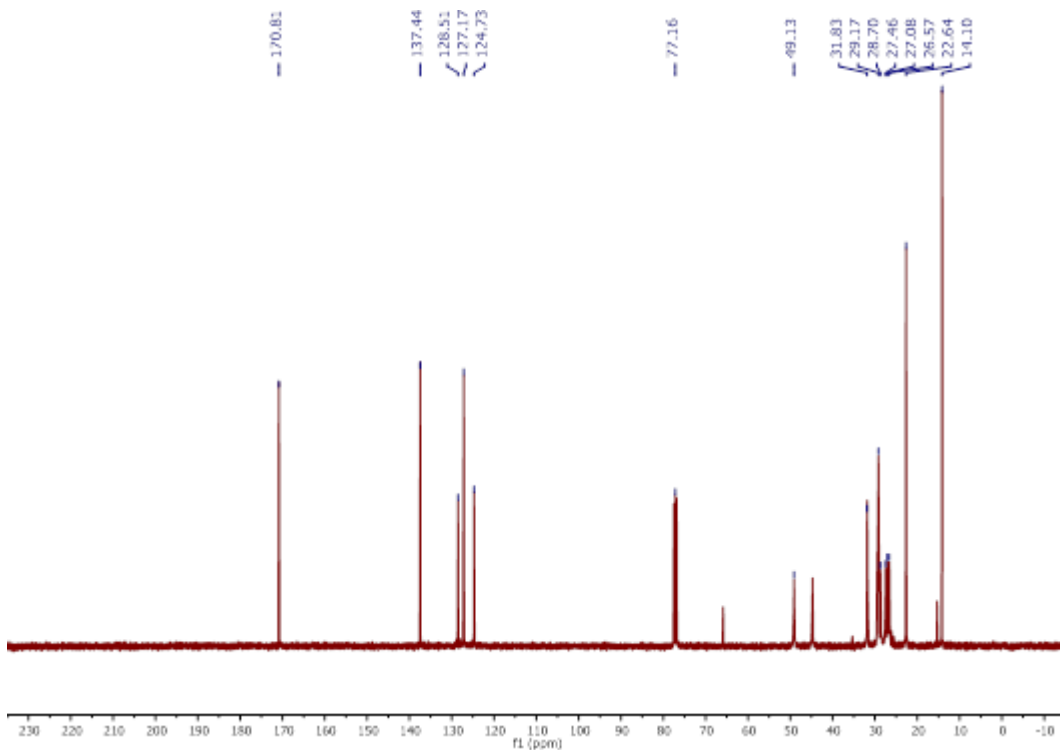


Figure S10. $^{13}\text{C}\{\text{H}\}$ NMR of 1,3-DOPA (*chloroform-d*, 100 MHz).

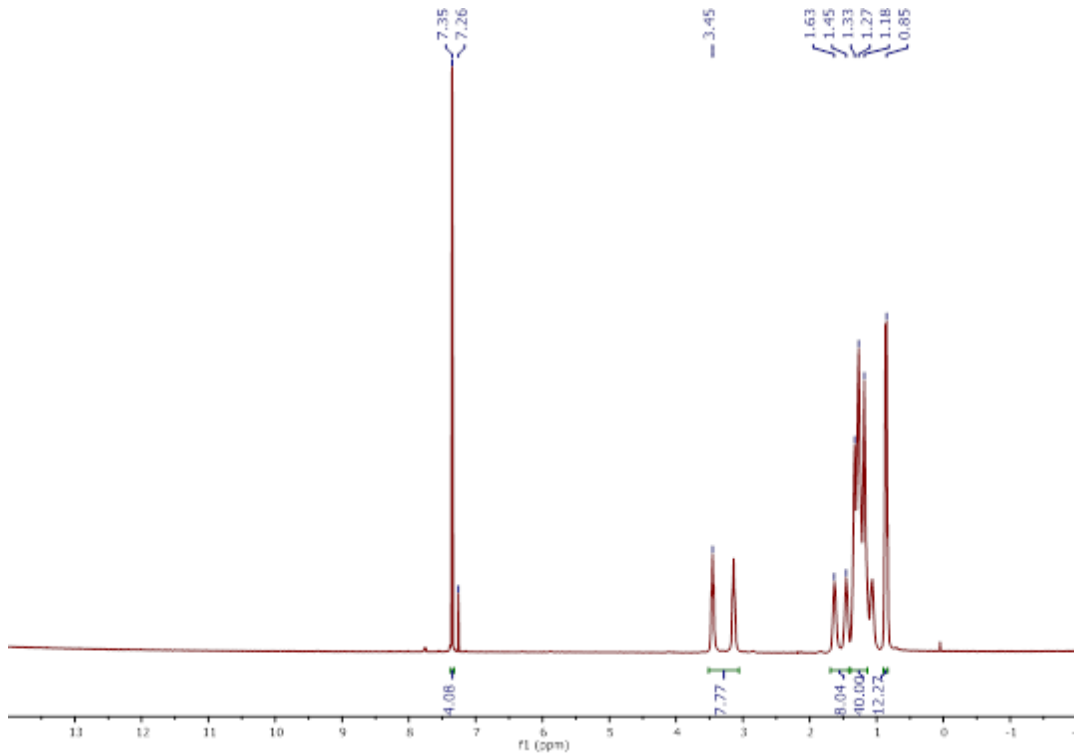


Figure S11. ^1H NMR of 1,4-DOPA (*chloroform-d*, 400 MHz).

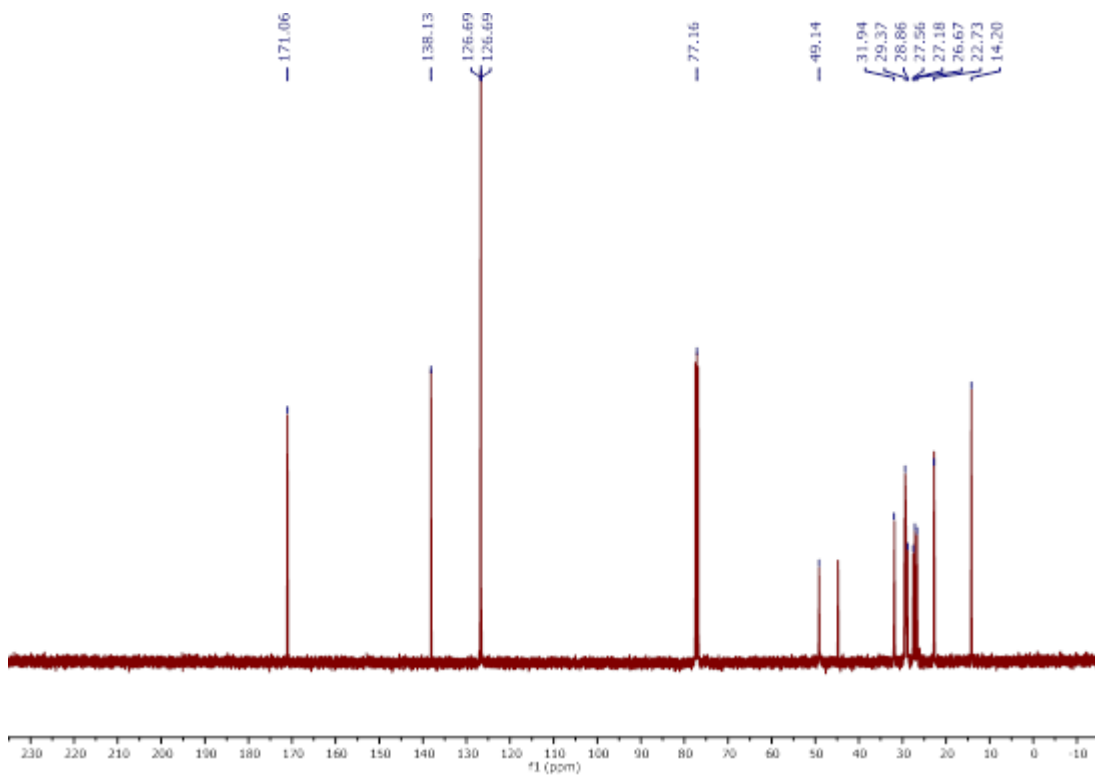


Figure S12. $^{13}\text{C}\{\text{H}\}$ NMR of 1,4-DOPA (*chloroform-d*, 100 MHz).

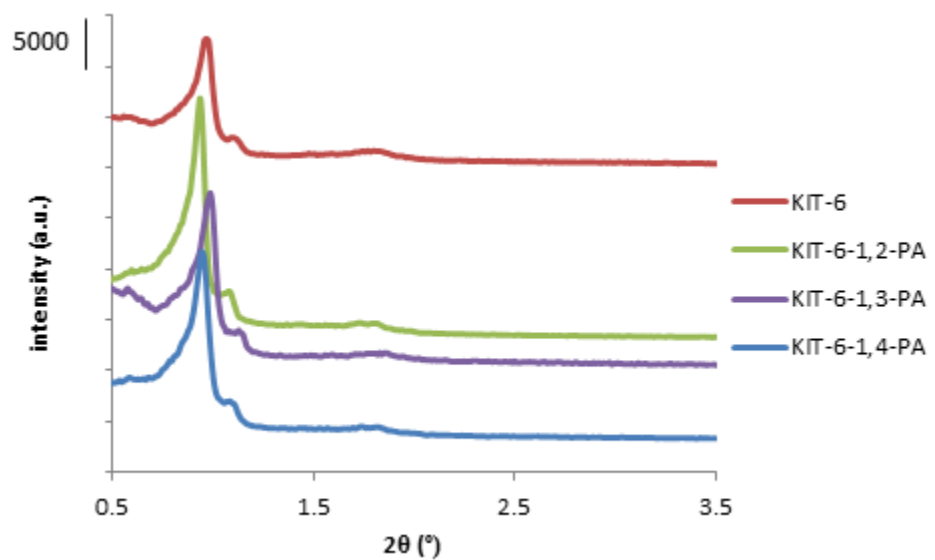


Figure S13. Low-angle powder XRD patterns of the pristine KIT-6 and the functionalized materials. Patterns are shifted upwards for clarity.

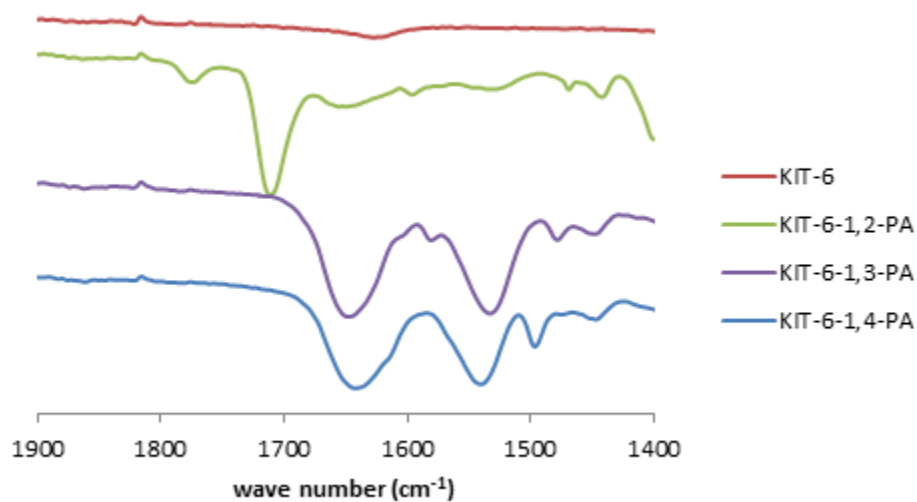
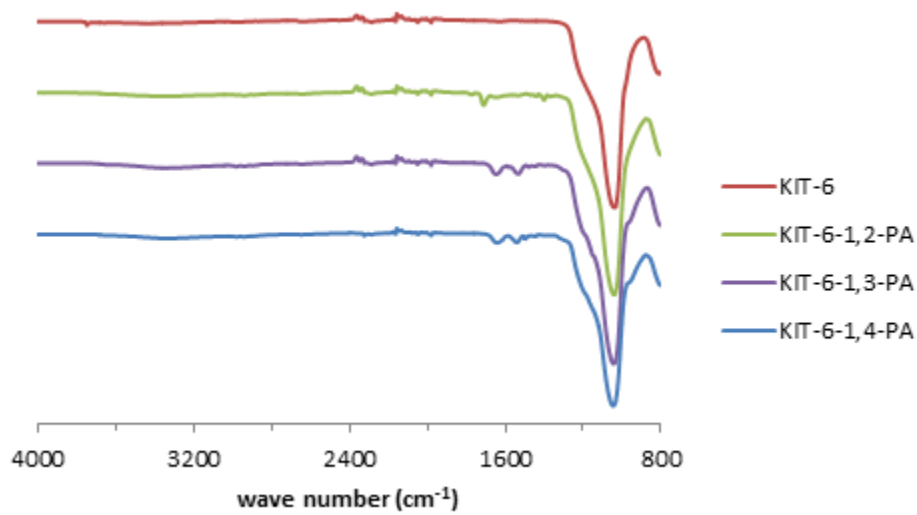


Figure S14. FTIR spectra of pristine mesoporous KIT-6 and all the functionalized KIT-6 samples (top) and enlarged zoom at 1400-1900 cm^{-1} (bottom). The spectra are normalized to the intensity of the SiO_2 band at 1041 cm^{-1} .

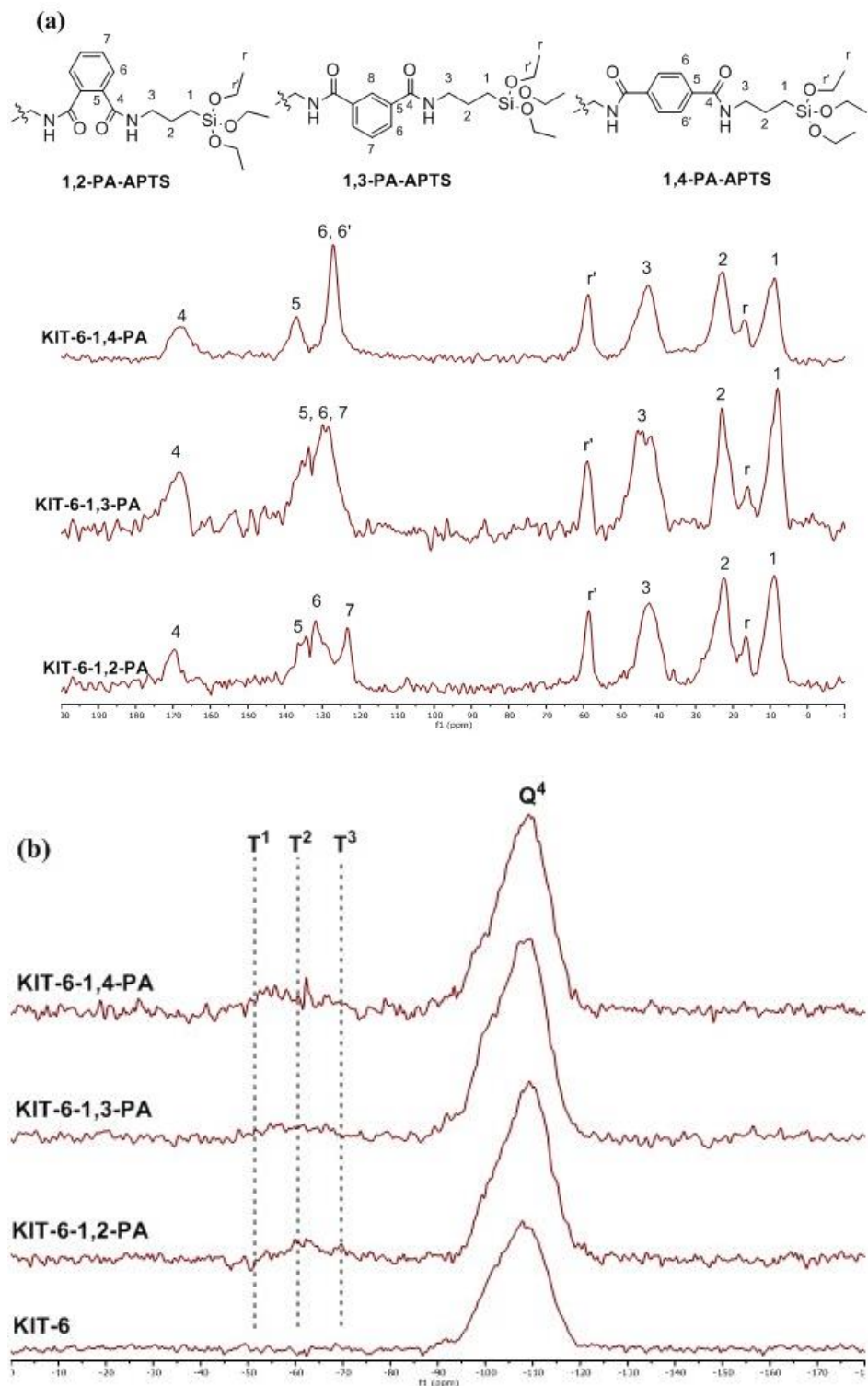


Figure S15. Solid state ^{13}C CP/NMR (a) and ^{29}Si MAS NMR (b) for the different functionalized mesoporous materials, as indicated.

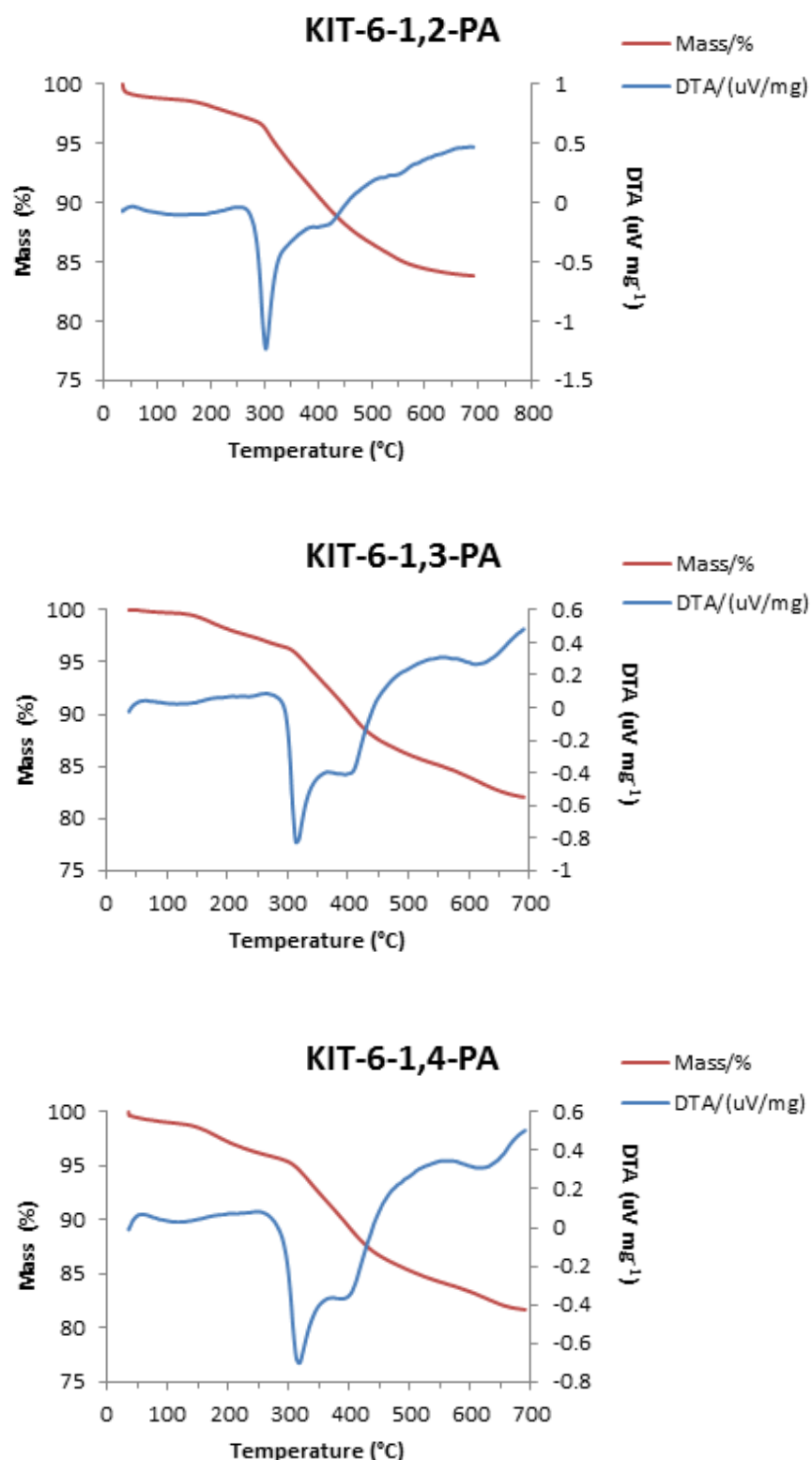


Figure S16. The thermogravimetric analysis (TGA, red) and differential thermal analysis (DTA, blue) curves of the ligand-modified KIT-6 silica samples (as indicated).

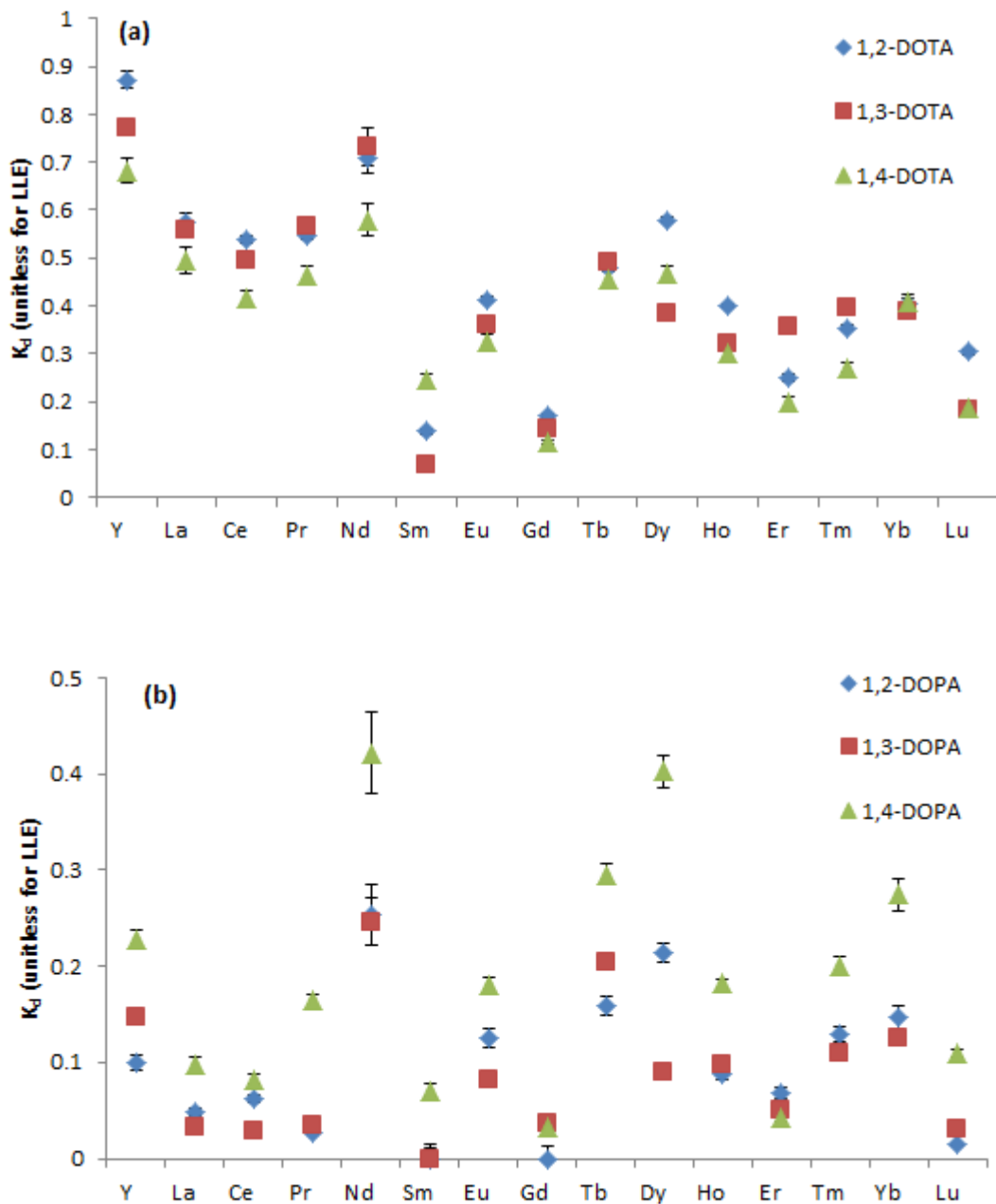


Figure S17. Distribution coefficient (K_d) values for 1,2-DOPA, 1,3-DOPA, and 1,4-DOPA in liquid-liquid extraction (LLE) using dichloromethane (a) and dodecane (b) as organic phase.

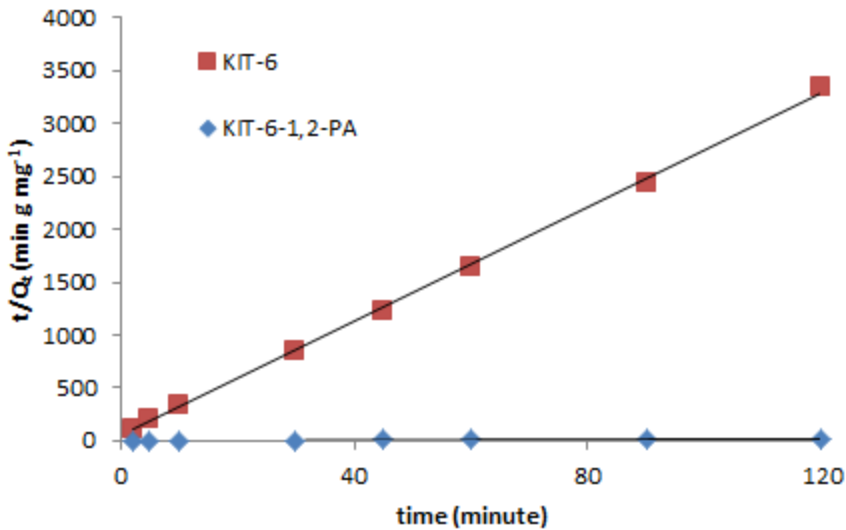


Figure S18. Linear regression of the pseudo-second-order kinetic model for adsorption of Lu³⁺ on mesoporous KIT-6 and KIT-6-1,2-PA sorbents.

The kinetic curves of KIT-6 and KIT-6-1,2-PA sorbents were fitted with pseudo-first-order (equation S1) and pseudo-second-order (equation S2) kinetic models as given below:

$$Q_t = Q_e - Q_e e^{-k_1 t} \quad (\text{S1})$$

$$Q_t = \frac{k_2 Q_e^2 t}{1 + k_2 Q_e t} \quad (\text{S2})$$

where Q_t (mg g⁻¹) and Q_e (mg g⁻¹) represent the amount of lutetium captured at time t , and at equilibrium, respectively, k_1 (L min⁻¹) and k_2 (g mg⁻¹ min⁻¹) are the rate constant of the pseudo-first-order and pseudo-second-order models. In addition, the half equilibrium time $t_{1/2}$ (min) of pseudo-second-order kinetic can be calculated according to equation S3:

$$t_{1/2} = \frac{1}{k_2 Q_e} \quad (\text{S3})$$

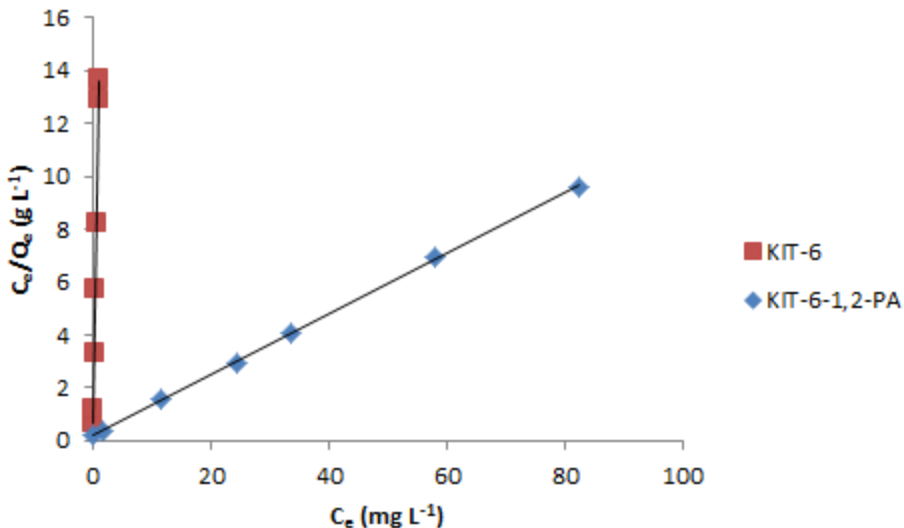


Figure S19. Linear regression of the Langmuir isotherm model of KIT-6 and KIT-6-1,2-PA used for the adsorption isotherms experiments.

The equations of the Langmuir (equation S4) and Freundlich (equation S5) isotherm models were expressed as follows:

$$Q_e = \frac{K_L Q_m C_e}{1 + K_L C_e} \quad (\text{S4})$$

$$Q_e = K_F C_e^{1/n} \quad (\text{S5})$$

where C_e (mg L⁻¹) stands for the equilibrium concentration, and Q_e (mg g⁻¹) is the adsorption capacity at equilibrium. Q_m (mg g⁻¹) represents the maximum adsorption capacity of the materials. K_L (L g⁻¹) is the affinity constant, and K_F (mg g⁻¹) represents the adsorption capacity direction constant, and 1/n indicates favorable adsorption condition.

For the Langmuir model, the separation factor (or equilibrium parameter constant) R_L can be obtained from the following equation S6:

$$R_L = \frac{1}{1 + C_m K_L} \quad (\text{S6})$$

where C_m (mg g⁻¹) is the maximum initial concentration.

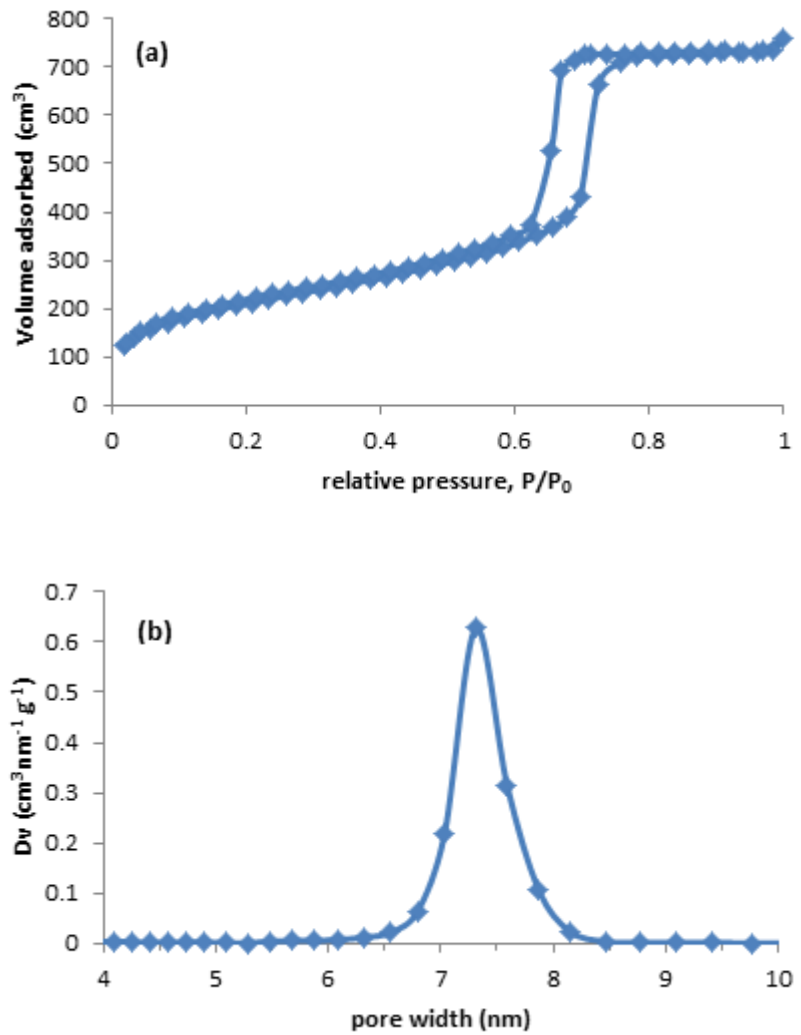


Figure S20. (a) N_2 adsorption–desorption isotherm at $-196\text{ }^{\circ}\text{C}$ of KIT-6-1,2-PA sample after the reusability test and (b) respective NLDFT pore size distribution.

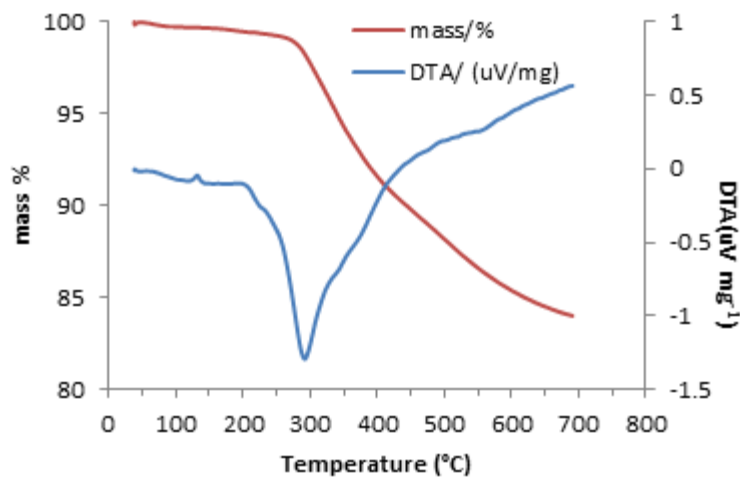


Figure S21. TGA (red) and DTA (blue) curves of KIT-6-1,2-PA sample after the reusability test.

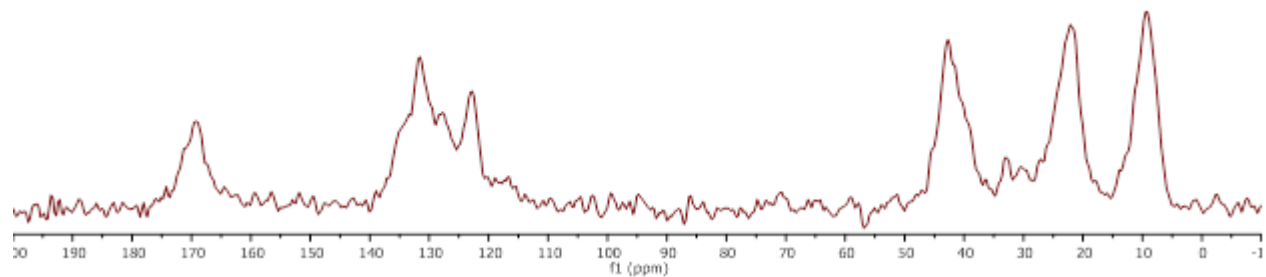


Figure S22. ¹³C CP/MAS NMR spectrum of KIT-6-1,2-PA after the reusability test.

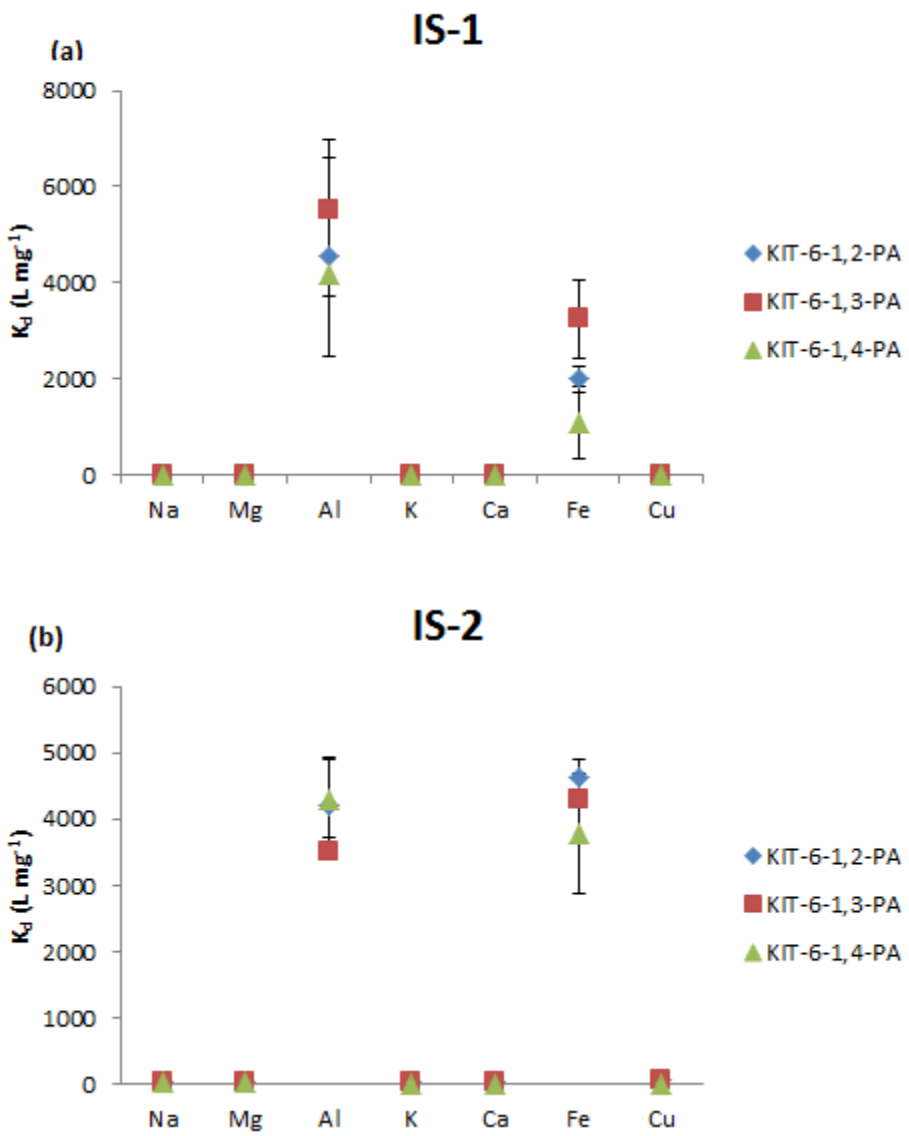


Figure S23. Distribution coefficient (K_d) values of functionalized hybrid materials for competitive ions in industrial samples IS-1 (a) and IS-2 (b).

Table S1. Adsorption equilibrium constants for Langmuir and Freundlich isotherm models.

Material	Langmuir				Freundlich			
	Q _{m,exp} (mg g ⁻¹)	K _L (L mg ⁻¹)	Q _{m, cal} (mg g ⁻¹)	R _L	R ²	K _F (mg g ⁻¹)	1/n	R ²
KIT-6-1,2-PA	8.47	0.599	8.69	0.0164	0.999	3.71	0.218	0.932
KIT-6	0.0595	60.46	0.0598	0.0181	0.999	0.0622	0.110	0.981

Table S2. Tabulated distribution coefficients (K_d) values for solid-phase extraction (SPE).

Element	SPE (KIT-6-PA material), mL g ⁻¹		
	1,2-PA	1,3-PA	1,4-PA
Y	12413	5998	8679
La	814	6561	7870
Ce	1575	18045	8059
Pr	2049	19358	8265
Nd	2084	22756	8501
Sm	4141	20488	8931
Eu	4689	7292	8959
Gd	3916	4055	8711
Tb	6971	2258	8674
Dy	10227	1677	8851
Ho	11679	1380	8703
Er	17604	1360	8773
Tm	33757	1646	8965
Yb	40488	1858	9864
Lu	53541	1834	9995
Al	1829	2270	2049
Fe	1227	1478	1352

Table S3. Tabulated distribution coefficients (K_d) values for liquid-liquid extraction (LLE) using dichloromethane and dodecane as organic phase.

element			LLE				
	1,2-DOPA dichloromethane	1,2-DOPA dodecane	1,3-DOPA dichloromethane	1,3-DOPA dodecane	1,4-DOPA dichloromethane	1,4-DOPA dodecane	
Y	0.872	0.10	0.773	0.14	0.682	0.23	
La	0.575	0.05	0.560	0.03	0.494	0.09	
Ce	0.540	0.06	0.494	0.02	0.418	0.08	
Pr	0.547	0.03	0.564	0.04	0.465	0.16	
Nd	0.707	0.25	0.732	0.24	0.579	0.42	
Sm	0.139	0.00	0.069	0.00	0.245	0.07	
Eu	0.414	0.12	0.362	0.08	0.325	0.18	
Gd	0.172	0.00	0.142	0.03	0.115	0.03	
Tb	0.481	0.16	0.491	0.20	0.456	0.29	
Dy	0.579	0.21	0.386	0.09	0.466	0.40	
Ho	0.401	0.09	0.323	0.09	0.303	0.18	
Er	0.251	0.07	0.355	0.05	0.198	0.04	
Tm	0.354	0.13	0.398	0.11	0.271	0.20	
Yb	0.405	0.15	0.388	0.12	0.406	0.27	
Lu	0.304	0.01	0.184	0.03	0.187	0.11	

Table S4. Tabulated major elemental composition of diluted industrial mining wastes IS-1 and IS-2.

IS-1			IS-2		
REE ($\mu\text{g L}^{-1}$)	Competitive ions ($\mu\text{g L}^{-1}$)		REE ($\mu\text{g L}^{-1}$)	Competitive ions ($\mu\text{g L}^{-1}$)	
Y	85.78	Na	961.14	Y	66.18
La	974.08	Mg	491.19	La	4164.2
Ce	2136.08	Al	955.42	Ce	7067.71
Pr	213.20	K	936.2	Pr	749.32
Nd	744.28	Ca	347.55	Nd	2524.99
Sm	95.02	Fe	1.86	Sm	242.41
Eu	5.54	Cu	16.5	Eu	57.99
Gd	67.95			Gd	169.53
Tb	6.79			Tb	10.97
Dy	25.95			Dy	27.83
Ho	4.61			Ho	3.68
Er	9.50			Er	7.81
Tm	2.21			Tm	1.54
Yb	5.49			Yb	1.68
Lu	1.23			Lu	0.30
total	4377.71	total	3711.96	total	15096.14
				total	102613.90

Table S5. Tabulated distribution coefficients (K_d) values for real-world samples.

SPE (KIT-6-PA material), mL g ⁻¹						
Element	1,2-PA		1,3-PA		1,4-PA	
	IS-1	IS-2	IS-1	IS-2	IS-1	IS-2
lanthanides						
Y	1053.77	4256.24	4256.24	1187.74	92.75	71.39
La	16.72	27.12	4591.18	1640.02	205.04	58.73
Ce	71.27	155.37	7970.05	2853.57	331.41	59.89
Pr	83.98	176.84	3654.18	2781.42	314.21	64.65
Nd	93.79	184.25	11980.41	3665.75	435.18	69.93
Sm	240.69	592.44	9814.73	364.60	302.75	78.18
Eu	324.72	781.84	781.84	550.80	362.37	82.27
Gd	215.16	483.00	483.00	293.92	233.19	79.65
Tb	349.03	763.73	763.73	414.47	342.89	60.44
Dy	995.83	3141.91	3141.91	1083.86	853.80	77.36
Ho	589.74	789.90	789.90	477.71	413.14	57.50
Er	1964.91	1142.68	1142.68	773.06	604.40	85.08
Tm	329.34	108.23	108.23	104.66	99.71	53.24
Yb	29199.85	15948.32	339.76	472.67	453.23	23.01
Lu	66263.31	20329.99	435.50	333.01	144.89	50.88
Competitive ions						
Na	0.00	31.64	0.00	31.29	0.00	22.93
Mg	0.00	27.41	12.67	31.40	17.47	22.10
Al	4544.18	4202.41	5533.93	3512.14	4173.47	4310.33
K	0.00	31.71	0.00	32.09	0.00	16.56
Ca	0.00	22.63	0.00	25.79	0.00	13.50
Fe	1991.42	4629.62	3242.56	4298.70	1087.74	3777.40
Cu	0.00	59.62	11.65	64.06	12.41	17.43